Tribology International 88 (2015) 298–308

Contents lists available at ScienceDirect

Tribology International

journal homepage: www.elsevier.com/locate/triboint

Gearbox power loss. Part I: Losses in rolling bearings

Carlos M.C.G. Fernandes [a,*], Pedro M.T. Marques [a], Ramiro C. Martins [a], Jorge H.O. Seabra [b]

[a] INEGI, Universidade do Porto, Campus FEUP, Rua Dr. Roberto Frias 400, 4200-465 Porto, Portugal
[b] FEUP, Universidade do Porto, Rua Dr. Roberto Frias s/n, 4200-465 Porto, Portugal

ARTICLE INFO

Article history:
Received 25 July 2014
Received in revised form
20 October 2014
Accepted 20 November 2014
Available online 3 December 2014

Keywords:
Rolling bearings
Gearboxes
Power loss
Wind turbine gear oils

ABSTRACT

This work is devoted to the analysis, modeling and validation of gearbox power loss, considering the influence of the gears, rolling bearings and seals, the influence of the operating conditions, lubricant formulation and the lubrication method.

The first part of this work a rolling bearing torque loss model is calibrated for several wind turbine gear oils and for ball and roller contacts. The results achieved clarify the importance of a rolling bearing in a gearbox power loss.

In the second part of this work will be presented the same approach for gears. The final part will converge in the application of findings in two full gearboxes, a planetary and a parallel axis gearbox, both in multiplying configuration.

1. Introduction

Wind turbines use wind energy to generate electricity, having nowadays a significant contribution to the electrical power generation from renewal sources around the world [1]. The blades of a wind turbine rotate at very low speeds, typically 20 revolutions per minute, which is not suitable for conventional power generation using an electrical generator. This problem is solved using a multiplying gearbox between the blades shaft and the generator. The gearbox might have different configurations, although one of the most used designs has two planetary stages plus a helical gear stage at the end. The efficiency of these multiplying gearboxes, with this arrangement or a similar one, is good. Nevertheless, any efficiency increase will have a significant impact, reducing the power loss and the operating temperature. In the case of 1 MW wind turbine an improvement of 0.34% in efficiency per gear stage, could lead to a reduction of 10 kW in power loss and a reduction of the operating temperature above 5 °C. Besides the additional power produced, the reduction in operating temperature contributes to a better lubrication, less oil degradation and lower needs in maintenance. Such increase in gearbox efficiency is already possible through an improved gear tooth design or selecting the most suitable gear oil formulation, or even, combining these two possibilities. Furthermore, gear oils generating lower gear power loss will have a similar effect on rolling bearings supporting the gearbox shafts. It is clear that the comparison of different wind turbine gear oil formulations, in terms of power loss and operating temperature, in gears and rolling bearings, can be very useful to understand and predict the efficiency and the operating temperature of a wind turbine gearbox.

According to Hohn et al. [2], as well as several other authors [3–14] the power loss in a gearbox consists of gear (P_{VZ0} and P_{VZP}), bearing (P_{VL}), seals (P_{VD}) and auxiliary losses (P_{VX}) as presented in Fig. 1.

Gear and bearing losses can be separated in no-load (P_{VZ0}) and load losses (P_{VZP}). No-load losses occur with the rotation of mechanical components, even without torque transmission. No-load losses are mainly related to lubricant viscosity and density as well as immersion depth of the components on a sump lubricated gearbox, but it also depends on operating conditions and internal design of the gearbox casing. Rolling bearing losses depend on type and size, arrangement, lubricant viscosity and immersion depth; the oil formulation is also important.

Load dependent losses occur in the contact of the power transmitting components. Load losses depended on the transmitted torque, coefficient of friction and sliding velocity in the contact areas of the components. Load dependent rolling bearing losses also depend on type and size, rolling and sliding conditions and lubricant type [15].

Full gearbox tests give very good indication of the operating temperature and total power loss, for a given set of operating conditions (input torque and speed), but it is very difficult to isolate the power loss corresponding to each component, gear set, rolling bearing or seal. Full gearbox tests also do not allow a clear separation between load and no-load dependent losses. In order to have good predictions of the power losses related to each component, dedicated tests are necessary, as well as accurate

* Corresponding author.
E-mail address: cfernandes@inegi.up.pt (C.M.C.G. Fernandes).

http://dx.doi.org/10.1016/j.triboint.2014.11.017
0301-679X/

Notation and Units

a	ASTM D341 reference kinematic viscosity (cSt)
d_m	rolling bearing mean diameter (mm)
Fa	axial load (N)
G_{rr}	factor depending on the bearing type, bearing mean diameter and applied load (/)
G_{sl}	factor depending on the bearing type, bearing mean diameter and applied load (N mm)
K_{rs}	starvation constant for oil bath lubrication (/)
K_Z	bearing type related geometry constant (/)
m	ASTM D341 viscosity parameter (/)
M_{exp}	bearing friction torque measured experimentally (N mm)
M'_{rr}	rolling friction torque (N mm)
M_{sl}	sliding friction torque (N mm)
M_{drag}	friction torque of drag losses (N mm)
M_{seal}	friction torque of seals (N mm)
M_t	internal bearing friction torque (N mm)
n	ASTM D341 viscosity parameter (/)
n	rotational speed (rpm)
R_1	geometry constant for rolling friction torque (/)
S_1	geometry constant for sliding friction torque (/)
s	piezoviscosity parameter (/)
t	piezoviscosity parameter (/)
α	piezoviscosity coefficient (Pa^{-1})
α_t	thermal expansion coefficient (/)
β	thermoviscosity coefficient [$°K^{-1}$]
η	dynamic viscosity (Pa s)
ϕ_{bl}	sliding friction torque weighting factor (/)
ϕ_{ish}	inlet shear heating reduction factor [/]
ϕ_{rs}	kinematic replenishment/starvation reduction factor (/)
μ_{bl}	coefficient of friction in boundary film lubrication (/)
μ_{EHD}	coefficient of friction in full film lubrication (/)
μ_{sl}	sliding coefficient of friction (−)
μ	bearing coefficient of friction (−)
ν	kinematic viscosity (cSt)
ρ	density (g/cm^3)

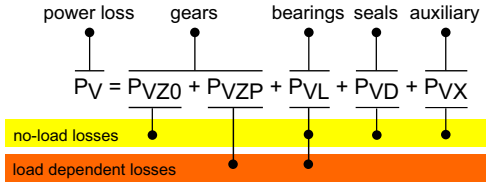

Fig. 1. Power loss contributions [3].

prediction models, that might be integrated in a general power loss model for gearboxes. The aim of the first part of this work is to calibrate a rolling bearing torque loss model, using the experimental results from tests performed with thrust ball bearings (TBB, elliptic contact) and cylindrical roller thrust bearings (RTB, line contact), lubricated with several wind turbine gear oils with different formulations.

2. Rolling bearing friction torque model

This model, proposed by SKF [15], considers that the total friction torque is the sum of four different physical sources of torque loss, represented by the following equation:

$$M_t = M'_{rr} + M_{sl} + M_{drag} + M_{seal} \quad (1)$$

The rolling bearings tested (see Table 1), TBB (51107) and RTB (81107), do not have seals and so the M_{seal} torque loss term was disregarded. The drag losses were very small because the operating speeds and the mean diameter of the rolling bearings are small and, consequently, the drag torque loss term was also disregarded. In Fig. 2 are presented the usual drag loss values for two different TBBs; two different RTBs, one NJ 406 cylindrical roller bearing and a four-point contact ball bearing. The results show that the rolling bearings tested here generated negligible drag losses. However, if rolling bearings with much higher diameter (TBB 51214 and RTB 81214) are used on the same conditions and if the rotational speed increases this term can be an important source of power loss. Since the TBB and RTB's that were used are quite small and operate at relatively low speeds the drag torque loss is negligible (Fig. 2).

Thus, the total internal friction torque of the rolling bearings has only two contributions: the rolling and sliding torques,

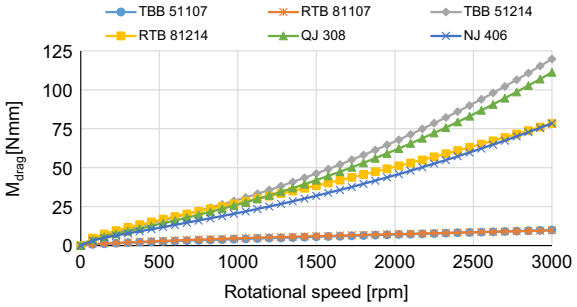

Fig. 2. Drag losses for different rolling bearing geometries. NJ 406 and QJ 308 under oil jet lubrication, the other geometries under half height oil bath for vertical shaft configuration lubricated with PAGD at 80 °C.

respectively, M'_{rr} and M_{sl}, as represented in the following equation:

$$M_t = M'_{rr} + M_{sl} \quad (2)$$

Eqs. (3)–(8) define the rolling and sliding torques,

$$M'_{rr} = \phi_{ish}.\phi_{rs}[G_{rr}(n.\upsilon)^{0,6}] \quad (3)$$

$$\phi_{ish} = \frac{1}{1 + 1.84 \times 10^{-9}(nd_m)^{1.28}\nu^{0.64}} \quad (4)$$

$$\phi_{rs} = \frac{1}{e^{K_{rs}\nu n(d+D)\sqrt{\frac{K_z}{2(D-d)}}}} \quad (5)$$

$$M_{sl} = G_{sl}.\mu_{sl} \quad (6)$$

The constants G_{sl}, G_{rr} are dependent on the geometry of the rolling bearing and are presented in Appendix A.

The sliding friction torque (Eq. (7)) is dependent on the weighting factor (Eq. (8)) and on the reference values of the coefficient of friction (boundary film coefficient of friction – μ_{bl} and full film coefficient of friction – μ_{EHD}) for each oil.

$$\mu_{sl} = \phi_{bl}.\mu_{bl} + (1 - \phi_{bl}).\mu_{EHD} \quad (7)$$

$$\phi_{bl} = \frac{1}{e^{2,6\times10^{-8}(n.\upsilon)^{1.4}d_m}} \quad (8)$$

The rolling bearing friction torque model, or torque loss model, only can predict accurate values if the boundary coefficient of friction μ_{bl} and the full film coefficient of friction μ_{EHD} are representative of the tested lubricant and of the operating temperature of the rolling bearing. For mineral oils, whatever the rolling bearing type, TBB or RTB, a value of $\mu_{bl} = 0.15$ is suggested by SKF [15]. Also for mineral oils a value of $\mu_{EHD} = 0.05$ is proposed for TBB, and a value of $\mu_{EHD} = 0.02$ is proposed for RTB [15].

There are no values of μ_{bl} and μ_{EHD} available for different gear oil formulations, neither for different operating temperatures. These values must be determined experimentally through rolling bearing tests.

3. Lubricants

Four fully formulated wind turbine gear oils, available in the market, a Mineral (MINR), a mineral mixed with PAMA (MINE), a Polyalkylene Glycol (PAGD) and a Poly-α-olefin (PAOR), were selected. The basic physical properties of these gear oils were determined (viscosity and density). These results are presented in Table 1.

The density of the different gear oils was measured at different temperatures using a DMA 35N densimeter. The thermal expansion coefficient [16] was calculated using those measurements.

The kinematic viscosities were measured using an Engler viscometer (according to *ASTM D341* [17]) at 40, 70 and 100 °C. All four lubricants (ISO VG 320) exhibited similar viscosities at 40 °C. At 100 °C significantly different viscosities were measured (see Table 1) which are in agreement with the differences in the corresponding Viscosity Index (VI).

In terms of additive packages, the ICP (chemical composition) suggests some differences within the fully formulated oils selected. The sulphur and phosphorus compounds, usually used in EP additives, appear in high concentrations in MINR, PAOR and MINE gear oils, while in PAGD they have significantly lower concentrations, mainly in what concerns to sulphur. The phosphorus content of PAGD is much higher than in the other formulations. Phosphorus can be used as an antioxidant in PAGD.

Table 1
Physical and chemical properties of wind turbine gear oils used.

Parameter Base oil	Unit (–)	MINR Mineral	PAOR Polialphaolefin	MINE Mineral + PAMA	PAGD Polyalkyleneglycol
Chemical composition					
Zinc (Zn)	(ppm)	0.9	3.5	< 1	1
Magnesium (Mg)	(ppm)	0.9	0.5	< 1	1.4
Phosphorus (P)	(ppm)	354.3	415.9	460	1100
Calcium (Ca)	(ppm)	2.5	0.5	2	0.8
Boron (B)	(ppm)	22.3	28.4	36	1.0
Sulphur (S)	(ppm)	11,200	5020	6750	362
Physical properties					
Density @ 15 °C	(g/cm^3)	0.902	0.859	0.893	1.059
Thermal expansion coefficient ($\alpha_t \times 10^{-4}$)	($°C^{-1}$)	−5.8	−5.5	−6.7	−7.1
Viscosity @ 40 °C	(cSt)	319.22	313.52	328.30	290.26
Viscosity @ 70 °C	(cSt)	65.81	84.99	93.19	102.33
Viscosity @ 100 °C	(cSt)	22.33	33.33	37.13	51.06
m	[/]	9.066	7.351	7.048	5.759
n	[/]	3.473	2.787	2.663	2.151
Thermoviscosity @ 40 °C ($\beta \times 10^{-3}$)	[$°K^{-1}$]	63.88	50.68	49.33	37.34
Thermoviscosity @ 70 °C ($\beta \times 10^{-3}$)	[$°K^{-1}$]	42.83	36.16	35.48	28.36
Thermoviscosity @ 100 °C ($\beta \times 10^{-3}$)	[$°K^{-1}$]	30.07	26.72	26.40	22.12
s @ 0.2 GPa	[/]	0.9904	0.7382	0.7382	0.5489
t @ 0.2 GPa	[/]	0.1390	0.1335	0.1335	0.1485
Piezoviscosity @ 40 °C ($\alpha \times 10^{-8}$)	[Pa^{-1}]	2.207	1.590	1.600	1.278
Piezoviscosity @ 70 °C ($\alpha \times 10^{-8}$)	[Pa^{-1}]	1.774	1.339	1.353	1.105
Piezoviscosity @ 100 °C ($\alpha \times 10^{-8}$)	[Pa^{-1}]	1.527	1.182	1.197	0.988
VI	[/]	85	150	163	230

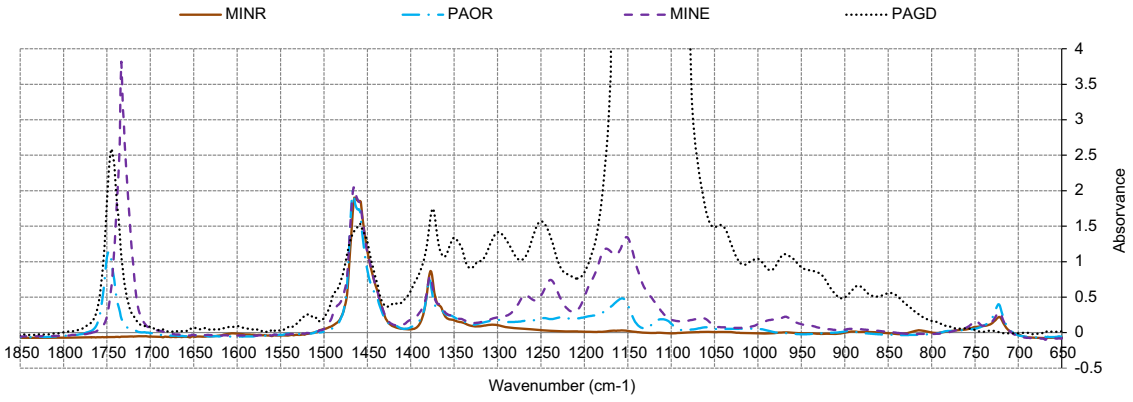

Fig. 3. IR (Infrared) spectra of the tested wind turbine gear oils.

Fig. 3 shows the IR spectra of the tested wind turbine gear oils, with several peak differences mainly in the "finger print" zone.

4. Test rig

The rolling bearing tests were performed on a modified Four-Ball machine, where the Four-Ball arrangement was replaced by a rolling bearing assembly, as shown in Fig. 4. This assembly was developed to test different rolling bearings and to measure the friction torque as well as the operating temperature in different points. A detailed presentation of this assembly can be found in [18].

As described in other works [18–22], four friction torque measurements were performed where three values are stored and the most dispersed disregarded. Due to the use of a piezo-electric sensor, the measurement should be made in a short period of time (less than 120 s) to avoid the "drift effect".

5. Calibration tests

In order to understand the behavior of the rolling bearing torque loss model a batch of rolling bearing tests was performed, under significant ranges of operating speeds and temperatures and using two types of rolling bearings, in all cases lubricated with PAOR gear oil. Table 2 summarizes the operating conditions used in these tests.

Fig. 5 shows the torque loss measured for each operating speed and temperature, for TBB (Fig. 5a) and RTB (Fig. 5b). For both rolling bearing types, and as expected [23,24], when the temperature increases (at constant speed) the torque loss decreases, within the temperature range considered (60 °C–80 °C).

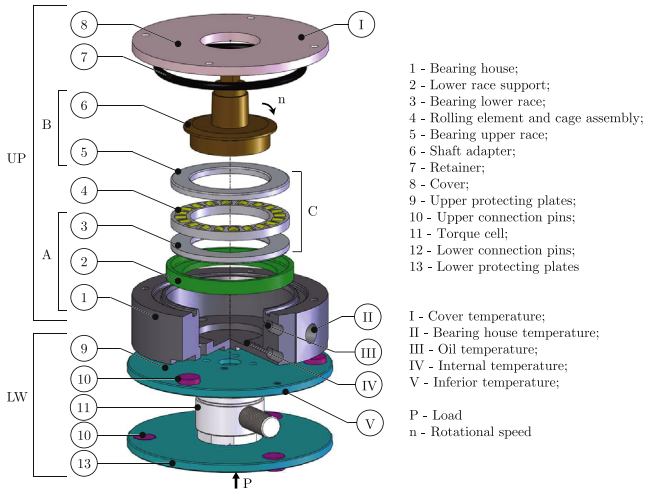

Fig. 4. Schematic view of the rolling bearing assembly.

In the case of the TBB 51107 when the speed increases (at constant temperature) the torque loss increases. However, at a very high temperature (e.g. 135 °C, see Fig. 5a) the opposite trend occurs. This different behavior is justified by the difference in lubrication regime when the temperature increases from 60 °C–80 °C to 135 °C. Using the viscosity ratio proposed by SKF [15], the viscosity ratio for 75 rpm is $\kappa=0.35$ at 80 °C and $\kappa=0.16$ at 135 °C. According to the literature the boundary lubrication starts for values of κ lower than 0.4.

In the case of 60, 70 and 80 °C it is important to assure that lubrication regime transition occurs in order to be possible to determine the boundary and full-film coefficient of friction.

In the case of the RTB 81107 the torque loss decreases when the speed increases (at a constant temperature), showing the opposite behavior of the TBB. Finally, comparing Fig. 5a and b, it is clear that the RTB generated significantly higher torque loss than the TBB, for the same conditions (e.g. 425 N mm for RTB vs 145 N mm for TBB, at 75 rpm and 80 °C).

Using the torque loss model proposed in Section 2 and considering that the total torque loss is equal to the experimental torque loss ($M_t = M_{exp}$), Eq. (1) can be written as

$$M_t = M_{exp} = M'_{rr} + M_{sl} \tag{9}$$

Calculating M'_{rr} using Eqs. (3)–(5), Eq. (9) becomes,

$$M_{sl} = M_t - M'_{rr} \tag{10}$$

and Eq. (10) gives

$$\mu_{sl}^{exp} = \frac{M_{sl}}{G_{sl}} = \frac{M_t - M'_{rr}}{G_{sl}} \tag{11}$$

Figs 5c and d shows the sliding coefficient of friction μ_{sl} for TBB and RTB, respectively. It is interesting to notice that in all cases, μ_{sl} decreases very slightly when the temperature increases and μ_{sl} also decreases when the operating speed increases. Furthermore, in the case of the RTB, μ_{sl} is almost temperature independent. Finally, it can be observed that μ_{sl} is smaller in the case of the RTB when compared to the TBB.

The influence of the lubrication regime can be clearly identified analyzing Fig. 5c for an oil temperature of 135 °C. At low speed ($n=75$ rpm), the boundary film lubrication regime prevails, and μ_{sl} reaches high values ($\mu_{sl}^{exp} \cong 0.07$) and at high speed (n=600 rpm) μ_{sl} is very small ($\mu_{sl}^{exp} \cong 0.025$) and the full film lubrication regime prevails.

Fig. 5e and f indicates that when speed and temperature increase the modified Stribeck parameter Sp [25] increases from 4×10^{-8} to 1×10^{-6} and the sliding coefficient of friction (μ_{sl}^{exp}) decreases from 0.055 to 0.037, in the case of TBB, and from 0.035 to 0.015 in the case of the RTB. These figures give a very good overview of the influence of the operating conditions on the sliding coefficient of friction for both types of rolling bearings, showing the interest of this modified Stribeck parameter [26].

Fig. 5e and f also indicates that the rolling bearing tests were performed under mixed film lubrication since a clear decrease of

Table 2
Operating conditions of calibration tests performed.

Operating conditions	Thrust ball bearing (TBB 51107)	Cylindrical roller thrust bearing (RTB 81107)
Mean diameter d_m (mm)	43.5	43.5
Number of elements (–)	21	20
Internal diameter d (mm)	35	35
Bore diameter D (mm)	52	52
Height H (mm)	12	12
Rotational speed (rpm)	75, 300, 900	75, 300, 600
Temperature (°C)	60, 70, 80, 135	60, 70, 80
Axial load (N)	7000	7000

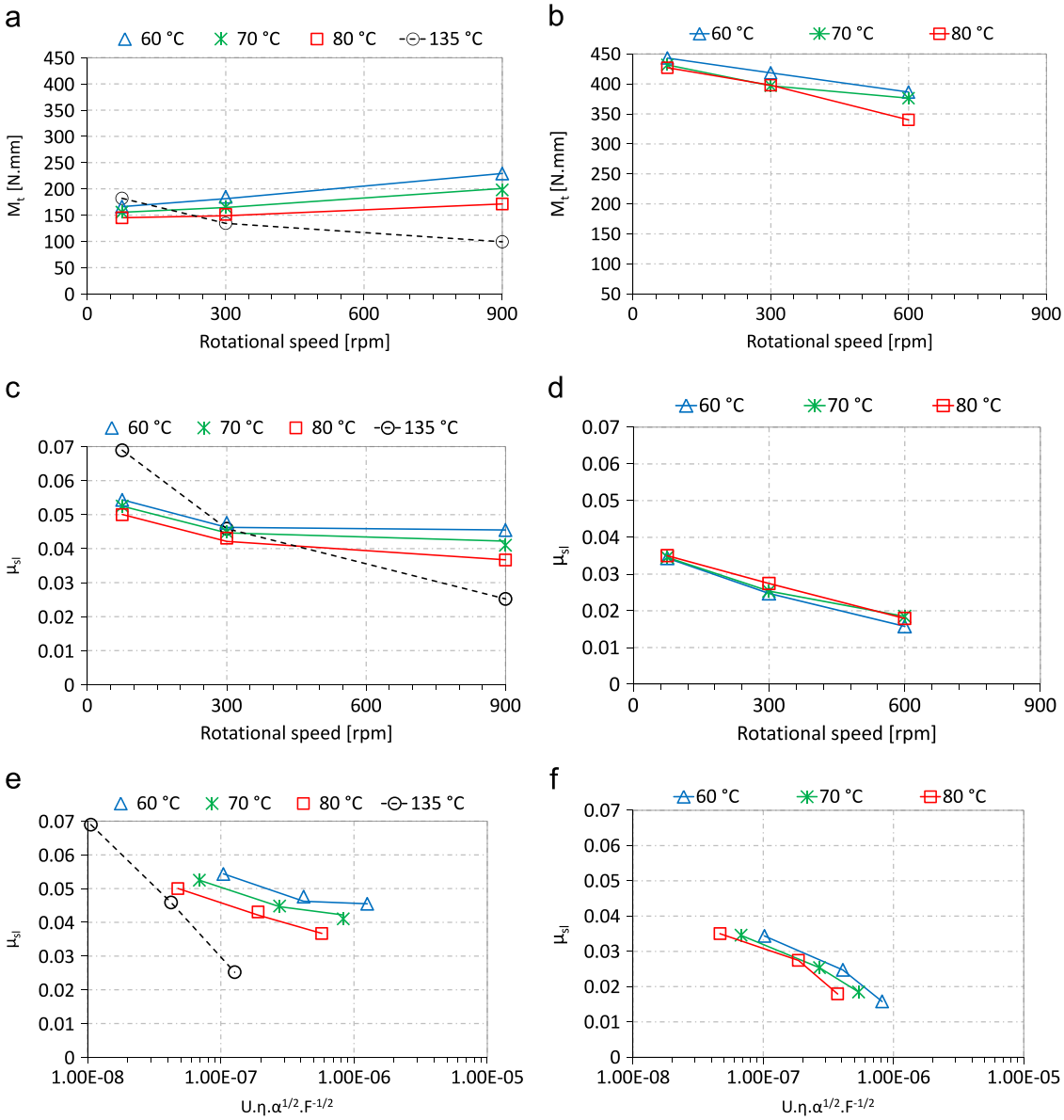

Fig. 5. Total friction torque (M_t) and sliding coefficient of friction (μ_{sl}) of a TBB and RTB rolling bearings under constant temperatures and an axial load of 7000 N. (a) TBB, (b) RTB, (c) TBB, (d) RTB, (e) TBB, and (f) RTB.

Table 3
Reference values of coefficient of friction, μ_{bl} and μ_{EHD} determined for the calibration tests with PAOR.

Temperature (°C)		TBB $3262.5 < n.d_m < 39,150$	RTB $3262.5 < n.d_m < 26,100$
60	μ_{bl}	0.059	0.044
	μ_{EHD}	0.046	0.016
70	μ_{bl}	0.055	0.046
	μ_{EHD}	0.042	0.015
80	μ_{bl}	0.052	0.043
	μ_{EHD}	0.037	0.014

the sliding coefficient of friction is observed when the modified Stribeck parameter increases.

Using Eqs. (10) and (11) of the torque loss model, it is possible to correlate the experimental values of the sliding coefficient of friction, μ_{sl}^{exp} shown in Fig. 5c and d, with the values of μ_{sl} predicted by Eq. (7).

We optimize μ_{bl} and μ_{EHD} in order to get the μ_{sl} from Eq. (7) the most close possible to experimental values μ_{sl}^{exp} calculated with Eq. (11). The values calculated are presented in Table 3 for each operating temperature and for each type of rolling bearing.

The values of μ_{bl} and μ_{EHD} are clearly dependent on the speed range used in the rolling bearing tests, as will be shown ahead. However, the values presented in Table 3 demonstrate that Eqs. (7) and (8) are totally suitable to accurately define the sliding coefficient of friction, for given operating conditions, if the values of μ_{bl} and μ_{EHD} are known for each lubricant, at a certain operating temperature, and a large range of operating speeds. The values presented in Table 3 also indicate that μ_{bl} and μ_{EHD} decrease when the temperature increases, as predicted by Brandão [26].

Using the values presented in Table 3 and Eqs. (7) and (8) it is possible to predict the sliding coefficient of friction, as shown by the solid line presented in Fig. 5c and d.

6. Sliding coefficient of friction of different rolling bearings lubricated with wind turbine gear oils

In order to evaluate the performance of other wind turbine gear oil formulations (MINR, MINE, PAGD, see Table 1), as well as the corresponding sliding coefficient of friction μ_{sl}, tests were performed at a constant temperature of 80 °C and under self-induced temperature (free temperature).

The tests were performed under an axial load of 7000 N and a speed range between 75 rpm and 1500 rpm, both for TBB and RTB.

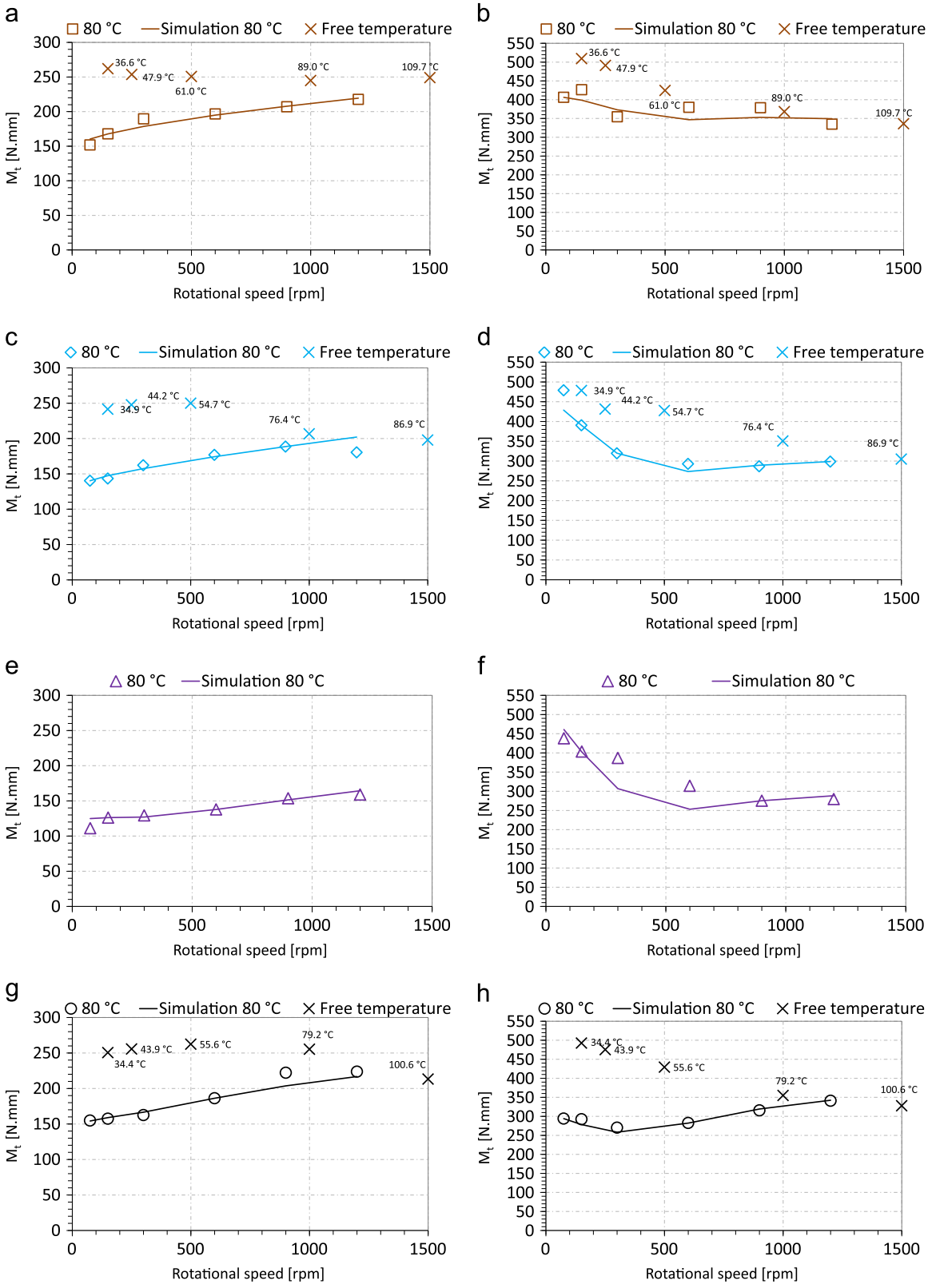

Fig. 6. Experimental of friction torque against rotational speed for a TBB and a RTB. (a) TBB and MINR, (b) RTB and MINR, (c) TBB and PAOR, (d) RTB and PAOR, (e) TBB and MINE, (f) RTB and MINE, (g) TBB and PAGD, and (h) RTB and PAGD.

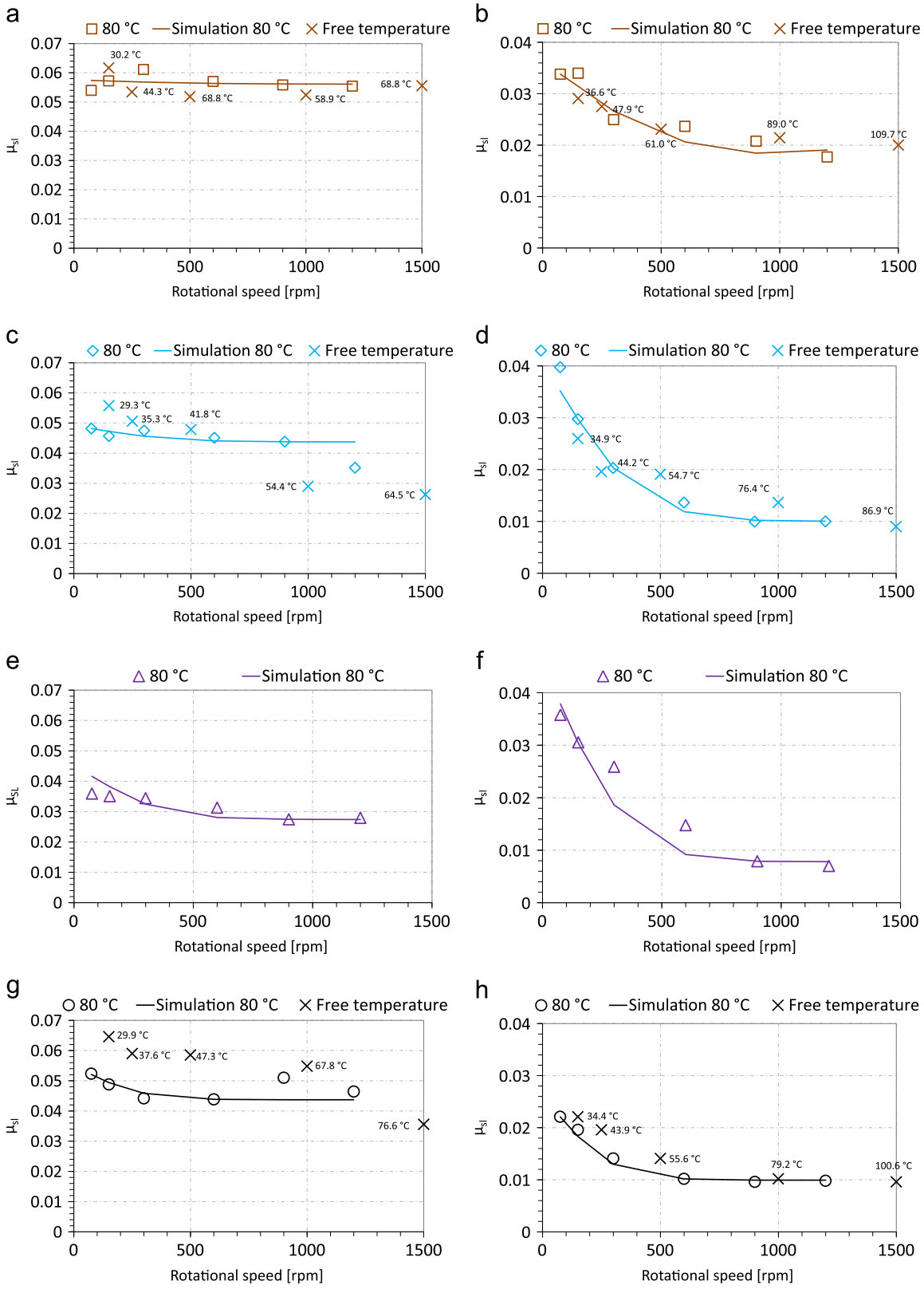

Fig. 7. Sliding coefficient of friction against rotational speed for a TBB and a RTB. (a) TBB and MINR, (b) RTB and MINR, (c) TBB and PAOR, (d) RTB and PAOR, (e) TBB and MINE, (f) RTB and MINE, (g) TBB and PAGD, and (h) RTB and PAGD.

The values of the torque loss (M_t^{exp}) are presented in Fig. 6 and the corresponding values of sliding coefficient of friction μ_{sl}^{exp} are presented in Fig. 7.

The results presented in Fig. 6 indicate that the rolling bearing torque loss (M_t^{exp}) is strongly dependent on the gear oil formulation and on the rolling bearing type. Under a constant temperature of 80 °C, and for TBB, the MINR formulation generated the highest torque loss while MINE formulation generated the lowest torque loss. The other two gear oil formulations, PAOR and PAGD, generated a torque loss between the previous two.

For RTB the MINR formulation generated again the highest torque loss, but the lowest torque loss was produced by the PAGD gear oil. At high speed (900 rpm and 1200 rpm) the formulations PAOR, MINE and PAGD generated very similar rolling bearing torque losses. In Fig. 6 the torque losses for the tests performed under self-induced temperature are also presented, as well as the corresponding operating temperature. These results have already been presented and analyzed in references [19,27].

Using Eq. (11) and the same procedure described earlier, the experimental torque loss (M_t^{exp}) was used to calculate the corresponding sliding coefficient of friction μ_{sl}^{exp}, which are presented in Fig. 7, both for the tests under constant temperature and self-induced temperatures. It is interesting to notice that the values of μ_{sl}^{exp} for both tests are similar, although the values of self-induced temperature are in many cases significantly different from 80 °C. Significant differences between constant and self induced temperature tests were only observed for the TBB lubricated with PAGD gear oil formulation, as shown in Fig. 7g.

The sliding coefficient of friction (μ_{sl}^{exp}) can also be plotted against the modified Stribeck parameter as shown in Fig. 8, for both types of rolling bearings, TBB and RTB, and for a constant temperature of 80 °C. As expected when the Stribeck parameter increases the sliding coefficient of friction (μ_{sl}^{exp}) in general decreases.

As in the previous section, μ_{bl} and μ_{EHD} were calculated minimizing the difference between experimental and numerical values of the sliding coefficient of friction, this time only for the tests at 80 °C, but covering a larger range of the operating speed (75 rpm up to 1200 rpm), and for all gear oil formulations and the two rolling bearing types. The corresponding values of μ_{bl} and μ_{EHD} are presented in Table 4.

At 80 °C, and within the speed range considered (75 rpm $\leq n \leq$ 1200 rpm), RTB always generated lower boundary film and full film coefficients of friction than TBB. The boundary coefficient of friction, μ_{bl}, depends on the gear oil formulation, as shown in Table 4. The author do not tested the values for other conditions different from $3262.5 < n \cdot d_m < 52,200$.

In the case of the TBB the highest values were obtained with the MINR and PAGD formulations, and the lowest values with the PAOR and MINE formulations. Exactly the opposite trend was obtained in the case of the RTB.

The full film coefficient of friction, μ_{EHD}, also depends on the gear oil formulation and rolling bearing type. For RTB there is a clear difference between the mineral oil (MINR), $\mu_{EHD} = 0.018$, and all the other formulations which have similar μ_{EHD} values, $0.008 \leq \mu_{EHD} \leq 0.010$. In the case of TBB such behavior of mineral and synthetic formulations is not observed. Using the values presented in Table 4 and Eqs. (7) and (8) it is possible to predict the sliding coefficient of friction, as shown by the solid lines in Figs. 7 and 8.

In Fig. 9 is presented a comparison between the calibrated model and the original SKF model with the suggested values of $\mu_{bl}=0.15$ and $\mu_{EHD}=0.05$ for a TBB both for constant temperature and free temperature conditions.

Fig. 10 shows a simulation for a load 10 times lower compared with the experimental results published in [24]. It can be stated that the

Table 4
Coefficient of friction of both TBB and RTB rolling bearings for an operating temperature of 80 °C.

	Speed	$3262.5 < n.d_m < 52,200$	
Oil	Bearing type	TBB	RTB
MINR	μ_{bl}	0.058	0.035
	μ_{EHD}	0.056	0.018
PAOR	μ_{bl}	0.049	0.039
	μ_{EHD}	0.044	0.010
MINE	μ_{bl}	0.044	0.044
	μ_{EHD}	0.027	0.008
PAGD	μ_{bl}	0.054	0.025
	μ_{EHD}	0.044	0.010

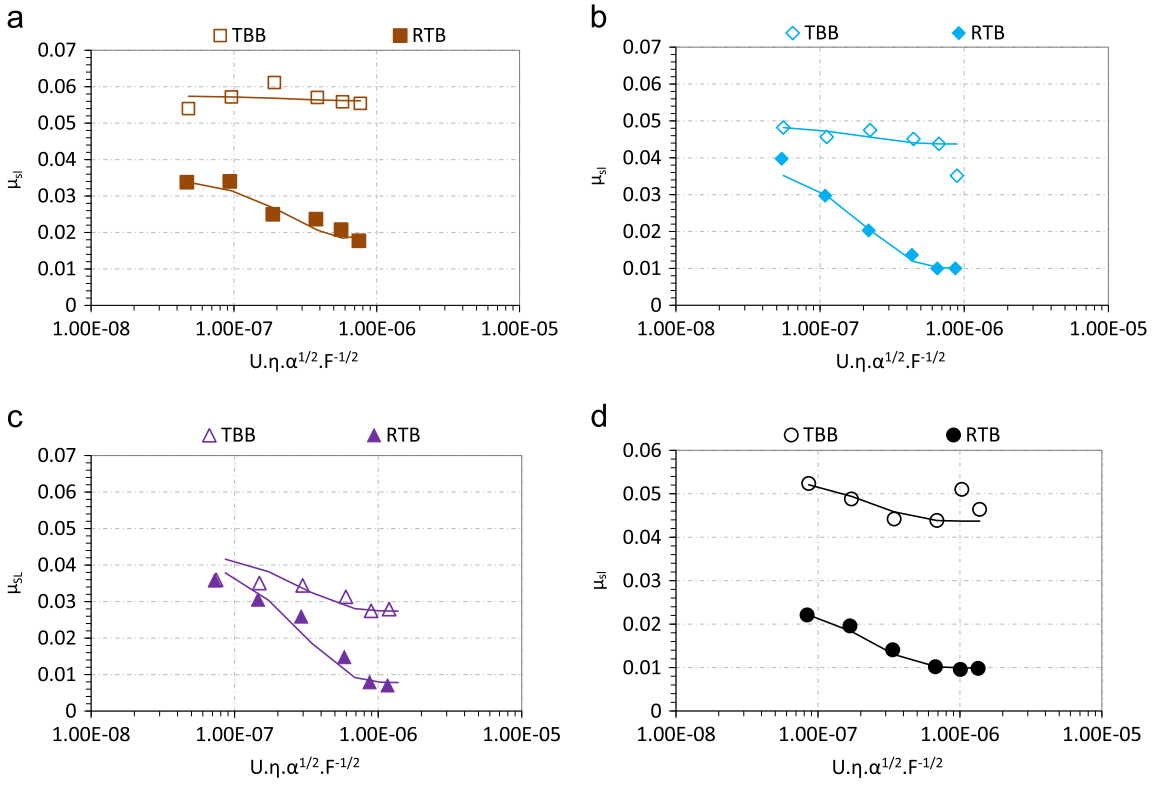

Fig. 8. Sliding coefficient of friction against modified Stribeck parameter for the TBB 51107 and RTB 81107 and corresponding model simulations with values of Table 4 (solid lines). (a) MINR, (b) PAOR, (c) MINE, and (d) PAGD.

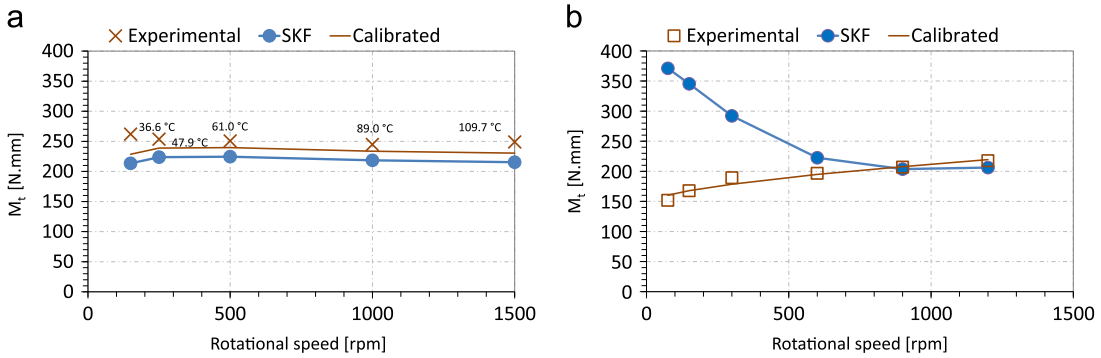

Fig. 9. Comparison of the original SKF model (μ_{bl}=0.15 and μ_{EHD} = 0.05) and calibrated model (Values for MINR on Table 4) for a TBB 51107. (a) TBB under free temperature conditions (MINR) and (b) TBB under constant temperature conditions (MINR).

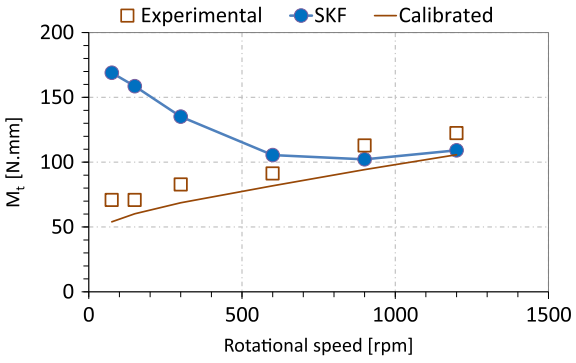

Fig. 10. Comparison of the original SKF model (μ_{bl}=0.15 and μ_{EHD} = 0.02) and calibrated model (Values for MINR on Table 4) for a RTB 81107 under 700 N. Experimental results published in [24].

Table 5
Rolling bearings assembled on the slave and test FZG gearboxes.

FZG Gearbox	Rolling bearings
Slave	4 NJ 406 cylindrical roller bearings
Test	2 NJ 406 cylindrical roller bearings + 2 QJ 308 four-point contact ball bearing

calibration done with 7000 N results keep valid for lower loads. It is advised to not use very light loads because the rolling bearing do not work properly and the model starts to deviate from the actual friction results.

7. Simulation of rolling bearings losses in a FZG gearbox

The values of μ_{bl} and μ_{EHD} (see Table 4), plus Eqs. (7) and (8) allow the definition of sliding coefficient of friction for any type of rolling bearing. In rolling bearings where the races and rolling elements generate elliptic contacts, the values corresponding to the TBB will be used. In the cases where line contacts are generated the values corresponding to the RTB are considered.

Thus, the torque loss model, can be extrapolated to any type of bearing operating in any type of gearbox. As an example the case of the test gearbox of the FZG machine will be considered.

The FZG machine, is usually used to perform gear tests, can test both spur and helical gear geometries. The drive gearbox has spur gears, only supports radial loads and uses cylindrical roller bearings (CRB). The test gearbox where both spur and helical gears can be tested, have both cylindrical roller bearings and four-point contact ball bearings (FCB) to balance the axial loads, as presented in Table 5.

Using the torque loss model and the corresponding coefficient of friction determined in the previous section at 80 °C (see Table 4), a simulation was performed for the cylindrical roller bearing and for the four-point contact ball bearing lubricated with each wind turbine gear oil formulation under jet-oil lubrication. The equations related to the geometry of these bearings are presented in Appendix A.

This simulation was performed considering the load stage K9 of the FZG machine (load arm length of 0.35 m) corresponding to an applied torque on the wheel of 323 Nm, and oil jet lubrication at 80 °C. In these conditions, the radial load on both rolling bearings (CRB and FCB) is the same and equal to 2393 N and the axial load on the FCB is equal to 1594 N. Under these operating conditions and for speeds between 200 rpm and 1800 rpm, the torque loss model (Eq. (2)–(8)) together with the μ_{bl} and μ_{EHD} values from Table 4, can be used to evaluate the rolling bearing friction torque in each bearing and in the test gearbox, as shown in Fig. 11.

The four-point contact ball bearing (FCB) generated a higher torque loss (M_t) than the cylindrical roller bearing (CRB) whatever the speed considered. The rolling torque (M'_{rr}) of the FCB is always lower than the rolling torque generated by the CRB. The major differences are observed on the sliding torque, since the FCB generates a sliding torque loss that can be up to 10 times higher than the sliding torque generated by CRB.

Regarding the oils, and for a constant operating temperature of 80 °C, the MINR promoted the lowest rolling torque for both geometries because it has the lowest Viscosity Index. At low speed, the four-point contact ball bearing promoted higher torque loss due to the sliding torque contribution, i.e. the sliding torque of that geometry is 10 times higher than for a cylindrical roller bearing. Considering the sliding torque, dependent on the coefficient of friction of each oil, the results show a lower value for the mineral oil with viscosity index improver (MINE), while the mineral oil (MINR) promoted the highest torque dependent on the coefficient of friction.

8. Conclusions

The rolling bearing results allow us to draw the following conclusions:

- The methodology presented seems to be effective to determine the values of μ_{bl} and μ_{EHD} from experimental results, for different gear oil formulations.
- Given correct values of μ_{bl} and μ_{EHD}, the model can accurately predict the torque loss of a rolling bearing.

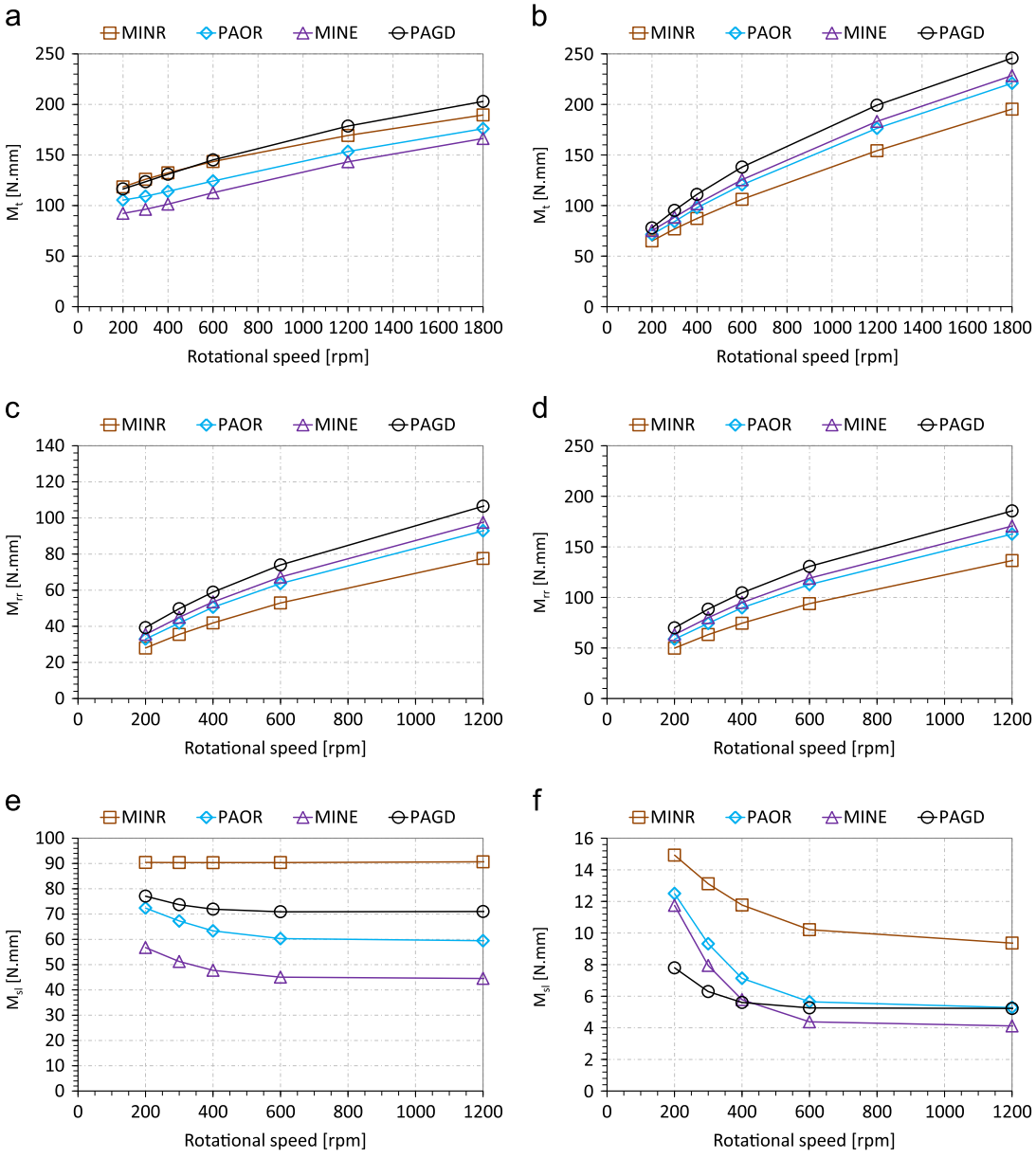

Fig. 11. Simulation for torque loss of a rolling bearing of a FZG test gearbox for a load stage K9 (323 Nm) with jet lubrication at 80 °C. (a) Four-point contact ball bearing, (b) cylindrical roller bearing, (c) four-point contact ball bearing, (d) cylindrical roller bearing, (e) four-point contact ball bearing, and (f) cylindrical roller bearing.

Table 6
SKF friction torque model constants for each rolling bearing geometry.

Oil	TBB	RTB	CRB	FCB
R1	1.03×10^{-6}	2.25×10^{-6}	1.09×10^{-6}	4.78×10^{-7}
R2	–	–	–	2.42
R3	–	–	–	1.40×10^{-12}
S1	1.6×10^{-2}	0.154	0.16	1.2×10^{-2}
S2	–	–	0.0015	0.9

- PAGD generated the lowest coefficient of friction for RTB.
- MINE generated the lowest coefficient of friction for TBB.

Acknowledgments

This work was funded by national funds through FCT – Fundação para a Ciência e a Tecnologia within the project EXCL/EMS-PRO/0103/2012.

Appendix A. SKF friction torque model

A.1. Thrust Ball Bearing (TBB)

$$G_{rr} = R_1 . d_m^{1.83} . F_a^{0.54} \tag{12}$$

$$G_{sl} = S_1 . d_m^{0.05} . F_a^{4/3} \tag{13}$$

A.2. Cylindrical roller thrust bearing (RTB)

$$G_{rr} = R_1 . d_m^{2.38} . F_a^{0.31} \tag{14}$$

$$G_{sl} = S_1 . d_m^{0.62} . F_a \tag{15}$$

A.3. Cylindrical Roller Bearing (CRB)

$$G_{rr} = R_1 . d_m^{2.41} . F_r^{0.31} \tag{16}$$

$$G_{sl} = S_1 . d_m^{0.9} . F_a + S_2 . d_m . F_r \tag{17}$$

A.4. Four-point Contact Ball Bearing (FCB)

$$G_{rr} = R_1.d_m^{1.97}.\left[F_r + F_g + R_2.F_a\right]^{0.54} \quad (18)$$

$$G_{sl} = S_1.d_m^{0.26}.\left[(F_r + F_g)^{4/3} + S_2.F_a^{4/3}\right] \quad (19)$$

$$F_g = R_3.d_m^4.n^2 \quad (20)$$

The model constansts for each rolling bearing geometry are presented in Table 6

References

[1] Europe's onshore and offshore wind energy potential—an assessment of environmental and economic constraints (European Environment Agency, 2009).

[2] Höhn B-R, Michaelis K, Vollmer T. Thermal rating of gear drives: balance between power loss and heat dissipation. AGMA Technical Paper.

[3] Höhn B-R, Michaelis K, Hinterstoißer M. Optimization of gearbox efficiency. goriva i maziva 2009;48(4):462–80.

[4] Hohn BR, Michaelis K, Wimmer A. Gearboxes with minimised power loss. VDI Berichte 2005(1904 II):1451–65.

[5] H´ohn B-R, Michaelis K, Otto H-P. Influence of immersion depth of dip lubricated gears on power loss, bulk temperature and scuffing load carrying capacity. Int J Mech Mater Des 2008;4(2):145–56.

[6] Michaelis K, Hohn BR. Influence of lubricants on power loss of cylindrical gears. STLE Tribol Trans 1994;37(1):161–7.

[7] Michaelis K. Die integraltemperatur zur beurteilung der fresstragf´ahigkeit von stirnr´adern [Ph.D. thesis, Dissertation]. TU M'´unchen; 1987.

[8] Changenet C, Velex P. A model for the prediction of churning losses in geared transmissions—preliminary results. J Mech Des 2007;129(1):128–33. http://dx.doi.org/10.1115/1.2403727.

[9] Changenet C, Velex P. Housing influence on churning losses in geared transmissions. J Mech Des 2008;130(6):062603. http://dx.doi.org/10.1115/1.2900714 URL ⟨http://link.aip.org/link/?JMD/130/062603/1⟩.

[10] Changenet C, Pasquier M. Power losses and heat exchange in reduction gears: numerical and experimental results. VDI Berichte 2002;2(1665):603–13.

[11] Changenet C, Leprince G, Ville F, Velex P. A note on flow regimes and churning loss modeling. J Mech Des 2011;133(12):121009. http://dx.doi.org/10.1115/1.4005330, URL ⟨http://link.aip.org/link/?JMD/133/121009/1⟩.

[12] Csoban A, Kozma M. Tooth friction loss in simple planetary gears. In: 7th international multidisciplinary conference, Baia Mare, Romania, May 17–18; 2007. p. 153–60.

[13] Martins R, Seabra J, Seyfert C, Luther R, Igartua A, Brito A. Power loss in FZG gears lubricated with industrial gear oils: biodegradable ester vs, mineral oil. In: Dowson MPGDD, Lubrecht AA, editors. Tribology and interface engineering series, vol. 48. Elsevier; 2005. p. 421–30.

[14] Martins RC, Cardoso NFR, Bock H, Igartua A, Seabra JHO. Power loss performance of high pressure nitrided steel gears. Tribol Int 2009;42(11–12):1807–15. http://dx.doi.org/10.1016/j.triboint.2009.03.006.

[15] SKF General Catalogue 6000 EN, SKF, November 2005.

[16] Denis J, Briant J. Hipeaux, Jean-Claude, Physico-Chimie dees Lubrifiants, Analyses et Essais, Publications de l'Institue Français du Pétrole, Éditions technip; 1997.

[17] Astm d341 - 09, standard practice for viscosity—temperature charts for liquid petroleum products.

[18] Cousseau T, Graça B, Campos A, Seabra J. Experimental measuring procedure for the friction torque in rolling bearings. Lubr Sci 2010;22(4 (April)):133–47.

[19] Fernandes CM, Martins RC, Seabra JH. Friction torque of cylindrical roller thrust bearings lubricated with wind turbine gear oils. Tribol Int 0 (2012). http://dx.doi.org/10.1016/j.triboint.2012.05.030.

[20] Fernandes CM, Amaro PM, Martins RC, Seabra JH. Torque loss in cylindrical roller thrust bearings lubricated with wind turbine gear oils at constant temperature. Tribol Int 2013;67(0):72–80. http://dx.doi.org/10.1016/j.triboint.2013.06.016, URL ⟨http://www.sciencedirect.com/science/article/pii/S0301679X13002363⟩.

[21] Fernandes CM, Amaro PM, Martins RC, Seabra JH. Torque loss in thrust ball bearings lubricated with wind turbine gear oils at constant temperature. Tribol Int 2013;66(0):194–202. http://dx.doi.org/10.1016/j.triboint.2013.05.002, URL ⟨http://www.sciencedirect.com/science/article/pii/S0301679X13002041⟩.

[22] Fernandes CM, Martins RC, Seabra JH. Friction torque of thrust ball bearings lubricated with wind turbine gear oils. Tribol Int 2013;58(0):47–54. http://dx.doi.org/10.1016/j.triboint.2012.09.005, URL ⟨http://www.sciencedirect.com/science/article/pii/S0301679X12003015⟩.

[23] Fernandes CM, Amaro PMP, Martins RC, Seabra JH. Torque loss in thrust ball bearings lubricated with wind turbine gear oils at constant temperature. Tribol Int (0) (2013) under review. http://dx.doi.org/10.1016/j.triboint.2012.05.030, URL ⟨http://www.sciencedirect.com/science/article/pii/S0301679X12001922⟩.

[24] Fernandes CM, Amaro PMP, Martins RC, Seabra JH. Torque loss in cylindrical roller thrust bearings lubricated with wind turbine gear oils at constant temperature. Tribol Int (0) (2013) under review. http://dx.doi.org/10.1016/j.triboint.2012.05.030, URL ⟨http://www.sciencedirect.com/science/article/pii/S0301679X12001922⟩.

[25] Brandão AJ, Meheux M, Ville F, CMJ, Seabra J. Traction curves and rheological parameters of fully formulated gear oils. Proc Inst Mech Eng Part J: J Eng Tribol 2011;225:577–93, http://dx.doi.org/10.1177/1350650111405111, in press.

[26] Brandão AJ, Meheux M, Ville F, CMJ, Seabra J. Traction curves and rheological parameters of fully formulated gear oils. Proceedings of the Institution of Mechanical Engineers, Part J: Journal of Engineering Tribology (in press) 2011;225:577–93.

[27] Fernandes CM, Martins RC, Seabra JH. Friction torque of thrust ball bearings lubricated with wind turbine gear oils. Tribology International 2013;58(0):47–54. http://dx.doi.org/10.1016/j.triboint.2012.09.005, URL ⟨http://www.sciencedirect.com/science/article/pii/S0301679X12003015⟩.